

Evaluation of Some Organic Compounds Containing O, N and S Atoms as Corrosion Inhibitors for Stainless Steel 304 in Acid Solutions

A. S. Fouada^{1,*}, M. A. Diab², A.Z. El-Sonbati² and Sh. A. Hassan¹

¹ Department of Chemistry, Faculty of Science, El-Mansoura University, El-Mansoura, 35516, Egypt, Tel: +2050 2365730; Fax: +2 050 2202271,

² Department of Chemistry, Faculty of Science, Damietta University, Damietta, Egypt

*E-mail: asfouda@hotmail.com

Received: 25 February 2017 / Accepted: 23 April 2017 / Published: 12 May 2017

The corrosion protection of stainless steel 304 (SS 304) in molar HCl solutions utilized by some organic compounds has been investigated by (WR) weight reduction, (EFM) electrochemical frequency modulation, (EIS) electrochemical impedance spectroscopy, (PP) potentiodynamic polarization tests and (AFM) atomic force microscope. It was found that inhibition rise with improving inhibitor dose and break down with temperature rising. The adsorption of organic compounds on SS 304 surface follows the Temkin's isotherm. PP experiments were performed at different solutions showed that these compounds act as mixed-kind inhibitors. Further, calculations of theoretical tests were occurred and correlations among experimental protection efficiency (% ω) and computed parameters were illustrated.

Keywords: Stainless steel 304; Corrosion inhibition; Hydrochloric acid; Organic compounds

1. INTRODUCTION

Stainless steel is corroded in acidic medium (HCl) [1, 2]. It is notable that corrosion never stops however its extension and seriousness can be brought down. But in fact it suffers from certain type of corrosion in some environments. The use of inhibitors is one of the most practical methods for protection against corrosion [3–5]. Organic assembled are usually utilized as corrosion protection to lessen the rate of corrosion in acidic media on stainless steel [6–9]. Protection effectiveness of organic assembled is ascribed for the most part to the nearness of a polar group going about as a adsorption active site. Adsorbed organic atoms avoid steel corrosion by hindering the site

active on the metal surfaces and the hindrance effectiveness (ω %) of an inhibitor relies on unequivocally on the chemical structure or the practical groups on the particle of inhibitor. A few works have concentrated the impact of organic assembled include nitrogen on the steel corrosion in acidic solution [10–21]. Several authors investigated the use of thiourea and thiourea derivatives as corrosion inhibitors in different media and in different metals [22-27]. Also, a number of authors studied the effect of glycine and its derivatives as corrosion inhibitors [28- 30].

The impact of this work was to discover the influence of inhibition and adsorption of various organic compounds containing O, N and S atoms in acidic medium on SS 304. Also, the temperature effect on the dissolution of SS 304 was investigated by WR, PP, EIS and EFM methods. Moreover, the relationship among parameters for quantum calculations and experimental protection efficiencies of the inhibitors was discussed.

2. EXPERIMENTAL

2.1. Materials preparation

SS 304 sheets have chemical compositions (wt.%): < 0.03 C, 18.0 Cr, 8.0 Ni and the rest iron were utilized as working electrode for all studies.

2.2. Chemical tests

The coins utilized were cutting to be a rectangular (20 x 20 x 3 ml). The coins were scratched with emery papers up to grade 2000 grit size. After being abraded then had washing in acetone, dried by filter paper. The coins were immersed in double distilled water and wiped dry before putting them in the solution test. After the coins were dipped in 100 ml of 1 M HCl attendance and lack of various doses organic assembled at unlike temperatures (25-55 °C). After different rinsed time the coins of SS 304 were obtain, washed with double distilled water and weighted after accurately dried. The ω % and θ were measured from:

$$\omega \% = 100 \times \theta = 100 \times [1 - (W / W^\circ)] \quad (1)$$

Where W and W° are mass reduction in the existence and nonexistence of assembled, continually.

2.3. Electrochemical techniques

PP researches were occurs at a rate of scan = 1 mV s⁻¹. The potential of electrode was maintains until reach stabilization after 35 min till a potential constant was arrived, which is defined as the OCP. PP diagrams for SS 304 coins in the test solution attendance and without unlike doses of organic assembled were listed from -1000 to 1000 mV at OCP. Then utilized i_{corr} was obtained from the ω calculation and (θ) as below:

$$\% \omega = \theta \times 100 = [1 - (i_{\text{corr}} / i_{\text{corr}}^\circ)] \times 100 \quad (2)$$

The EIS tests were done in the similar utilized for PP method given above. All EIS tests were occurs at OCP. The θ and PE given from EIS were measured by the following.

$$\omega\% = \theta \times 100 = \left[1 - \left(\frac{R_{ct}^{\circ}}{R_{ct}} \right) \right] \times 100 \quad (3)$$

Where R_{ct} and R_{ct}° are the resistances in the existence and nonexistence of organic assembled, continually.

EFM tests were take place by utilized 2 frequencies of 2 and 5 Hz. The intermodulation spectra include responses current assigned for harmonically and peaks intermodulation current. The higher peaks were utilized to measure CF-2 & CF-3 the causality factors, i_{corr} and β_c and β_a .

All the electrochemical tests were given by utilized the electrochemical workstation (Instruments Gamry PCI4-G750). The cell include ((SCE) saturated calomel electrode, the platinum was utilized as auxiliary electrodes and the electrodes for working constitute SS 304 coins of one cm^2 area.

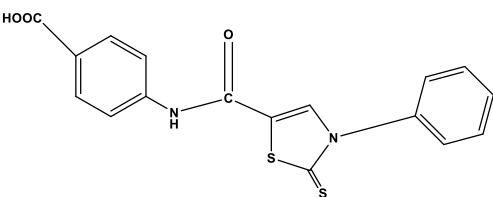
2.4. Surface analysis by atomic force microscopy (AFM)

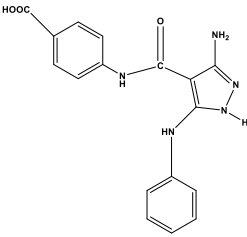
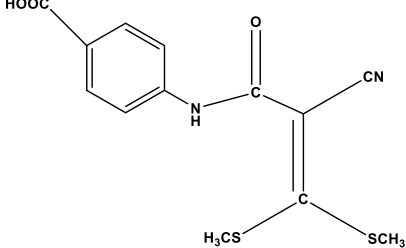
In this analysis the sample surface was scanned by a fine tip to find out surface morphology and properties to generate a 3D surface image and determine surface roughness, using SPM 2100 AFM instrument operating in contact mode in air. The scan rate size of all the AFM images is $05 \mu m \times 05 \mu m$ areas at a scan speed of $6.68 \mu m$ second.

2.5. Inhibitors

The aggressive acid solutions were carried out by dissolving an analytical (37%) grade HCl with double distilled water. All chemical used were given from Aldrich chemical company. Table 1 shows the molecular structures, names, molecular formulas and molecular weights of the organic assembled, which had been written by A, B and C.

Table 1. The structures, names, molecular weights and molecular formulas of investigated compounds

Comp	Structures	Names	Mol. Formulas	Mol. Wts
(A)		4-(3-phenyl-2-thioxo-2,3-dihydrothiazole-5-carboxamido)benzoic acid	$C_{17}H_{12}N_3O_3S_2$	371.43

(B)		4-(3-amino-5-(phenylamino)-1H-pyrazole-4-carboxamido)benzoic acid	$C_{17}H_{15}N_5O_3$	337.13
(C)		4-(2-cyano-3,3-bis(methylthio)acrylamido)benzoic acid	$C_{13}H_{12}N_2O_3S_2$	308.38

3. RESULTS AND DISCUSSION

3.1. Chemical techniques

3.1.1. Weight reduction (WR) tests

Table 2. CR in and ω value given from WR method for SS 304 in HCl in the nonexistence and existence of various doses of inhibitors at 25°C

Inhibitor concentration, μM	(A)	(B)	(C)
	% ω	% ω	% ω
1	30.0	19.7	15.4
5	50.6	30.4	21.8
10	56.4	44.9	30.8
15	65.1	54.1	39.7
20	78.2	65.4	56.7
25	91.0	76.2	66.2

WR tests for SS 304 were given in one M HCl in the nonexistence and existence of unlike doses of inhibitor up to 3 h at room temperature. The outcome data at various inhibitor doses are summarized in Table 1. Maximum doses of the inhibitor led to a break down in the data of the rate of corrosion, while the protection and the surface coverage rose. All the tests were obtained in the solutions naturally-aerated at either 25 °C or 55 °C utilized a condenser (thermostat-cooling) for the control of temperature. The coins were weighed after and before inundation, and mass reductions were measured. Values of % ω are recorded in Table 2. The data of protection efficiency improve with improving dose of inhibitor. This habit could be ascribed to the rise of the surface area coated by the molecules adsorbed organic assembled with the rise of its dose. At the same dose of inhibitors, the order of % ω was given as next: A > B > C.

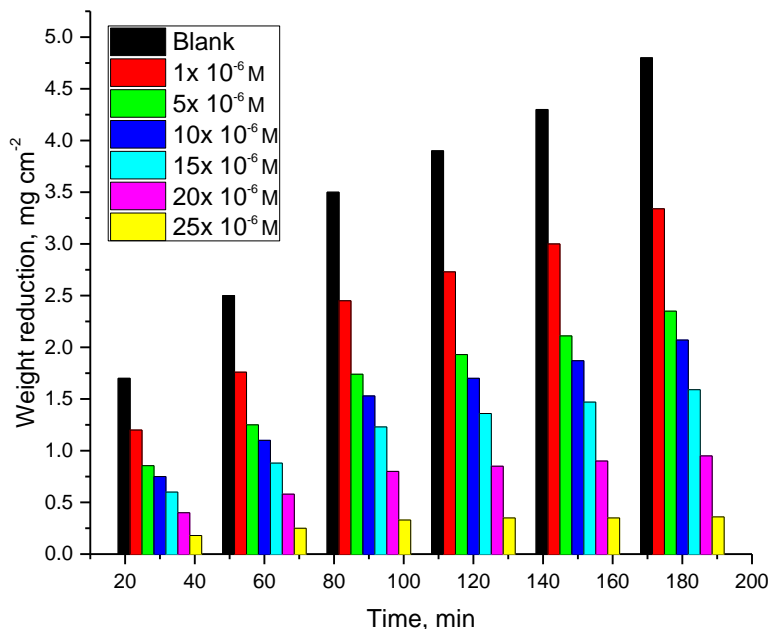


Figure 1. WR-time plots for the corrosion of SS 304 in the nonexistence and existence of different doses of inhibitor (A) in 1 M HCl at 25°C.

3.1.2. Adsorption behavior

The organic assembled adsorbed on the SS 304 surface is regarded as a adsorption substitution processes among the water adsorbed molecule on the SS 304 surface and organic composite in org_(aq) aqueous phase [31,32]:



Where n = number of molecules water eliminating from the 304 SS surface for each molecule of adsorbed inhibitor. Swinkless and Bockris [33], give (n) is assumed to be individual of coating or electrode charge. Clearly, the data of (n) will rely on the area of organic molecule cross-sectional with relation to that molecule of water.

In this section of the research, the data obtained of θ were fitted to different isotherms contain Frumkin, Langmuir, Flory-Huggins Temkin, Freundlich and Henry. The excellent fit was given by Temkin isotherm [34].

Table 3. Adsorption parameter for investigated inhibitors on 304 SS at various temperatures

Temp. °C	$K_{ads} \times 10^{-5} \text{ M}^{-1}$	$-\Delta G^{\circ}_{ads} \text{ kJ mol}^{-1}$	$-\Delta H^{\circ}_{ads} \text{ kJ mol}^{-1}$	$\Delta S^{\circ}_{ads} \text{ J mol}^{-1} \text{ K}^{-1}$
(A)				
25	5.14	49.3	24.4	79.6
35	3.26	50.7		
45	2.75	51.4		
55	2.00	52.2		
(B)				

25	2.71	47.3	28.7	62.0
35	2.25	48.1		
45	1.4	49.2		
55	0.94	49.3		
(C)				
25	20.49	44.5	30.4	53.8
35	1.41	44.8		
45	1.29	45.5		
55	0.84	46.2		

Plotting of log C against θ is show in Fig. 2 where relationships of line straight were given. The organic assembled adsorbed on 304 SS obeys perfectly adsorption Temkin.

$$\theta = 2.303/a \log C_{inh} + 2.303/a \log K_{ads} \quad (3)$$

Where C_{inh} = dose of inhibitor (M), (a) = factor draw the interaction molecular in the layer adsorbed and K_{ads} (M^{-1}) = equilibrium adsorption constant. The +ve data of (a) led to force attraction among the molecules adsorbed where the -ve data give forces repulsion among molecules adsorbed.

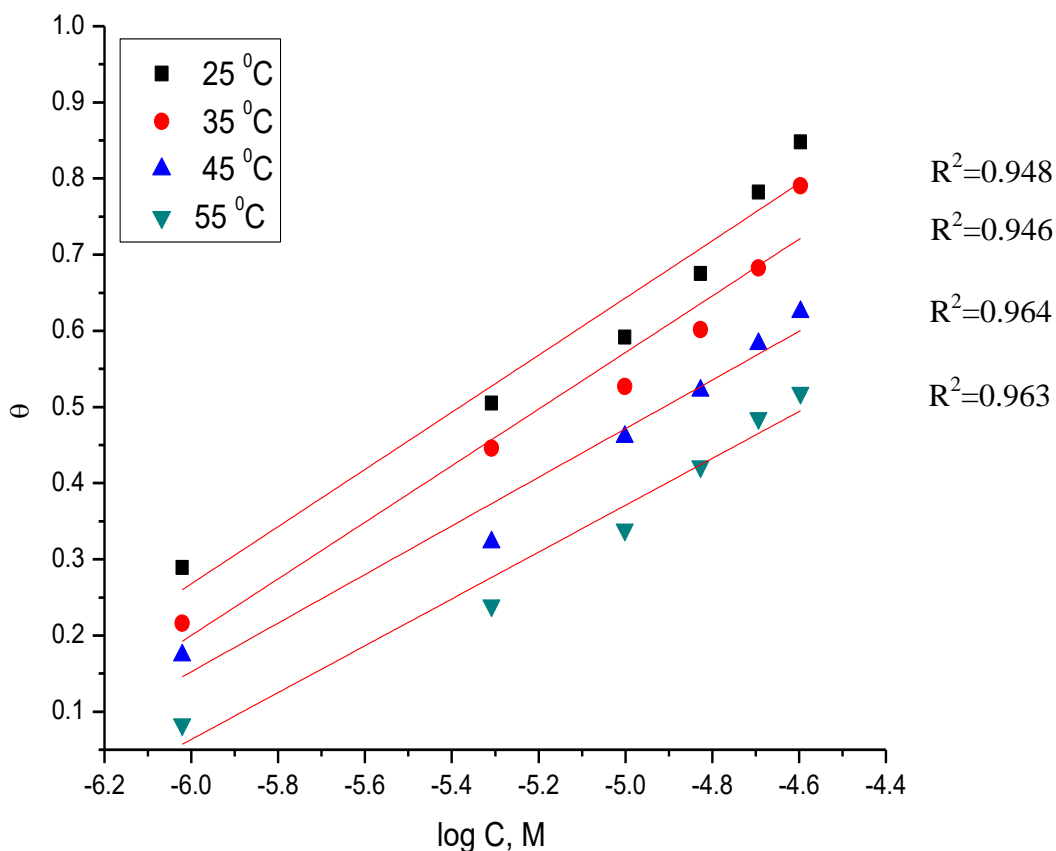


Figure 2. Temkin diagrams for SS 304 in existence and nonexistence of various doses of compound (A).

The ΔG°_{ads} was measured from the next equation [35]:

$$\Delta G^{\circ}_{ads} = - TR \ln (55.5 K) \quad (4)$$

Where $55.5 =$ water dose in solution (mol l^{-1}), $R =$ constant universal gas and $T =$ temperature absolute. By applying the equation $\Delta G^{\circ}_{\text{ads}} = \Delta H^{\circ}_{\text{ads}} - T \Delta S^{\circ}_{\text{ads}}$ and draw T against $\Delta G^{\circ}_{\text{ads}}$ relationships linear with intercept $=(\Delta H^{\circ}_{\text{ads}})$ and slope $= (-\Delta S^{\circ}_{\text{ads}})$ were given. The outcome value was listed in Table 3. From Table 3 we can obtain that:

- Data of K_{ads} lower with the temperature improve from 25 to 55 °C due to desorption of organic assembled from the 304 SS surface by higher temperature. This led to that these assembled are physically adsorbed on surface of 304 SS.
- The $-ve$ sign of $\Delta G^{\circ}_{\text{ads}}$ confirms the adsorption of inhibitors are spontaneous and strength of the thin film on the metal which lead to rise the disorder [36].
- The obtained $\Delta G^{\circ}_{\text{ads}}$ values were less negative than -40 kJ mol^{-1} led to the adsorption mechanism of the assembled components is chemisorptions as a result of the sharing or transfer of electrons from organic molecules to the 404 SS surface to form a bond coordinate [37]
- The $\Delta H^{\circ}_{\text{ads}}$ $-ve$ sign given that the exothermic adsorption process [38].
- $\Delta S^{\circ}_{\text{ads}}$ is $+ve$ sign of arises from substitution process [39], which indicates the rise in the solvent entropy. Given rise in disorder due to the fact that desorbed water molecules from the SS surface by inhibitor molecules.

3.1.3. Influence of temperature

The corrosion rate of SS 304 in free acid and in the existence of various doses of inhibitors was done in the range of temperature of 25–55°C utilized WR tests. The same diagrams to Fig.1 were given for other compounds (not shown). As the improve temperature, the rate of corrosion rises and hence the % ω of the compounds decreased. Due to desorption is obtained by improving temperature. These data given that the inhibitors adsorbed on surface of SS 304 take place among physical adsorption. The E_a , ΔH^* and ΔS^* for the SS 304 corrosion in nonexistence and existence of different inhibitors doses were measured from Arrhenius equation [40]:

$$k = A e^{(-E_a^*/RT)} \quad (5)$$

and equation transition [41]:

$$k = TR/Nh e^{(\Delta S^*/R)} e^{(-\Delta H^*/TR)} \quad (6)$$

where $T =$ temperature Kelvin, $k =$ rate of corrosion, $R =$ constant gas universal, $h =$ constant Planck's, $A =$ factor pre-exponential and $N =$ Avogadro's number.

Arrhenius plots of logarithmic values of $1/T$ (Kelven^{-1}) versus $\log k$ at dose constant of the organic assembled inhibitors, are given in Fig. 3 and $1/T$ vs. $\log(k/T)$, in Fig. 4 straight Lines with slope $= -\Delta H^*/2.303R$ and $-E_a^*/2.303R$, and intercepts $= \log R/Nh + \Delta S^*/2.303R$ and A for transition and Arrhenius equations, continually were given.

The obtained data of thermodynamic activation parameters (ΔG^* , ΔH^* , ΔS^*) for the dissolution of 304 SS in nonexistence and existence of organic assembled at different temperatures are recorded in Table 4. It is clear that E_a^* and ΔH^* vary in the similar manner for all tested compounds. So, the rate of corrosion is mainly decided by kinetic parameters of activation [43]. Also it is noted that the E_a^* is maximum in the existence of the tested compounds studied than in their nonexistence. The same data

were given by other authors [44-46]. The E_a^* values are helpful to determine the kind of adsorption. The maximum E_a^* values in the presence of the investigated compounds may be attributed to an appreciable lower in adsorption process of these investigated compounds on the SS 304 surfaces with rise in temperature [47].

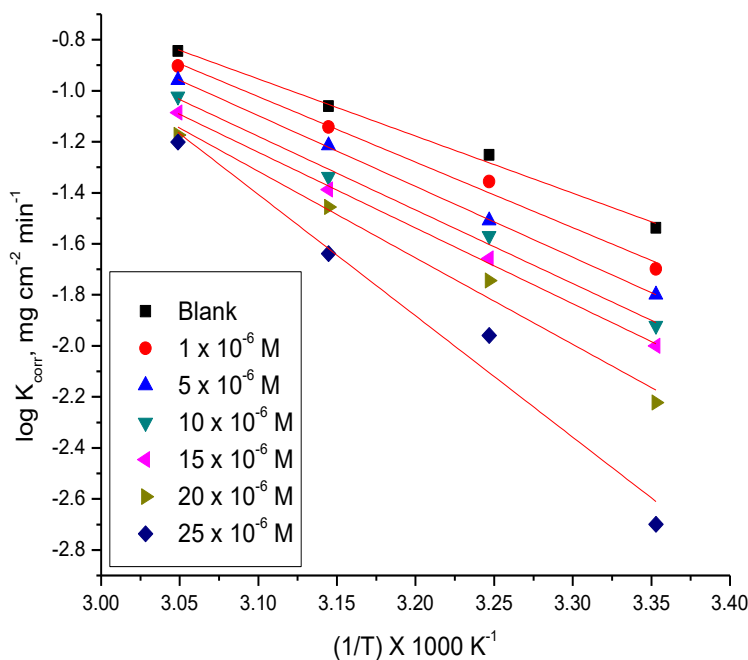


Figure 3. Arrhenius diagrams for SS 304 corrosion in the existence and nonexistence of various doses of compound (A).

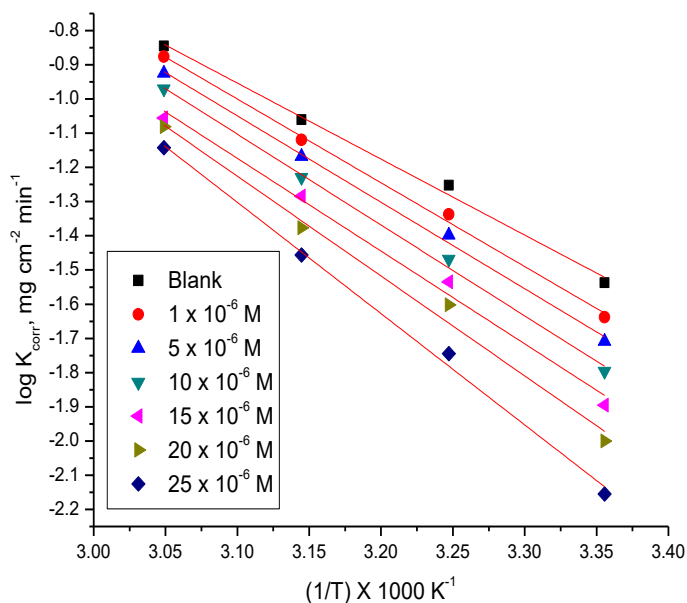


Figure 4. Transition state for dissolution of SS 304 in existence and nonexistence of various doses of compound (A)

Table 4. Thermodynamic activation parameters for dissolution of SS 304 in existence and nonexistence of various doses of investigated assembled.

Inhibitor	Conc. μM	E_a^* kJ mol^{-1}	ΔH^* kJ mol^{-1}	$-\Delta S^*$ $\text{J mol}^{-1} \text{K}^{-1}$
Blank	1.0 HCl	42.9	17.7	131.6
A	1	49.2	20.4	119.6
	5	53.1	22.3	107.4
	10	55.2	23.0	104.0
	15	56.8	23.7	100.2
	20	64.9	27.2	76.7
	25	91.1	31.7	46.4
B	1	61.9	62.7	125.8
	5	64.0	63.4	115.7
	10	68.6	64.0	112.6
	15	69.1	65.4	109.9
	20	69.3	66.0	102.3
	25	70.5	67.8	84.1
C	1	61.5	61.8	126.2
	5	63.0	62.3	124.3
	10	66.4	63.4	121.6
	15	66.80	65.10	120.1
	20	67.80	65.60	101.2
	25	68.70	66.40	100.7

Also, the rise (E_a^*) in presence of inhibitor compared to the blank given that the physically adsorption of the inhibitors on SS 304 surface while either unchanged or break down E_a^* in the presence of inhibitors suggest chemisorptions [48-49]. On second side, lower negative data of ΔS^* in the presence of the inhibitors, this means that presence of these assembled cause a lower in the disordering in direction from reactants to the complexes activated [50, 51]. The order of decreasing activation energy and thermodynamic parameters in the attendance of the organic assembled inhibitors agrees with the order of lowering IE% of these assembled.

3.2. Electrochemical techniques

3.2.1. PP tests

The breakdown of cathodic and anodic current density in attendance of investigated assembled Fig. 5 with improving dose. Similar curves had given for other inhibitors (not shown). PP diagrams were measured by the PP tests and the outcome parameters for example (R_p), (β_c , β_a), (η %), (i_{corr}), and (E_{corr}) were measured and recorded in Table 5. The numerical data of the deviation of the (β_a & β_c), i_{corr} , E_{corr} , θ and η_{Tafel} (%) were measured from equation 7 & are listed in Table 5.

$$\eta_{\text{Tafel}}\% = [1 - (i_{\text{corr}} / i_{\text{corr}}^0)] \times 100 \quad (7)$$

Where i_{corr} and i°_{corr} correspond to inhibit and non-inhibited corrosion current densities, respectively.

(E_{corr}) was given to change towards direction to more noble with the rise in the dose of inhibitor. The important of the 304 SS surface led to nature anodic of the investigated assembled. Cathodic Tafel slope (β_c) was obtain to lower at maximum inhibitor dose Table 5. This can be correlated with the lower in the transfer cathodic coefficient, which clearly led to the effect of investigated assembled on the kinetics of evolution reaction hydrogen [52].

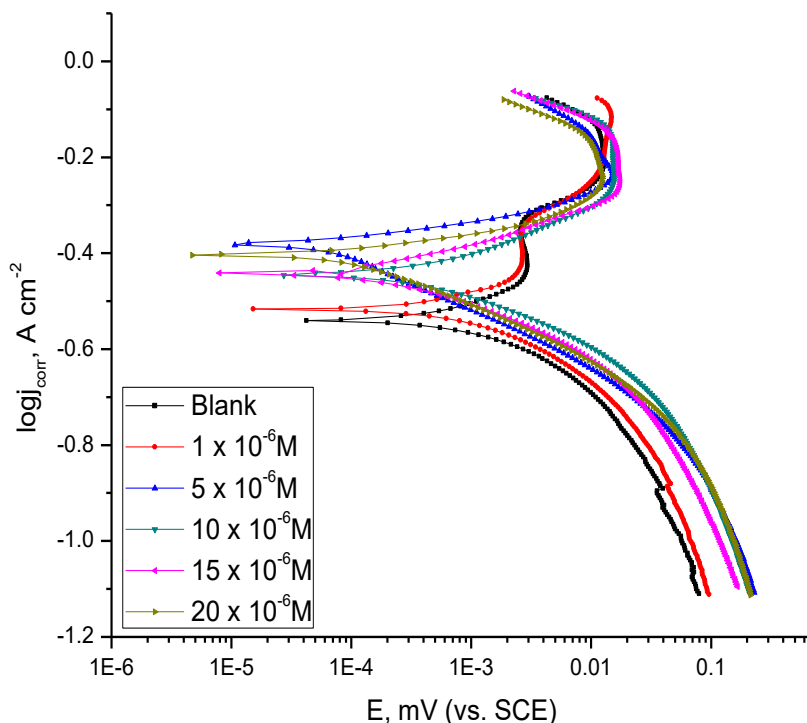


Figure 5. PP plots for the SS 304 corrosion of in nonexistence and existence of various doses of compound (A)

Table 5. Influence of inhibitors doses on the parameters of electrochemical from PP method for the SS 304 corrosion in HCl at 25°C

Inh.	Conc μ M	$-E_{\text{corr}}$, mV vs SCE	i_{corr} mA cm ⁻²	β_c mV dec ⁻¹	β_a mV dec ⁻¹	θ	% η	k_{corr}
Blank	0.0	540.0	930.0	109.5	173.9	-----	-----	424.8
A	1	517.0	673.0	99.2	121.0	0.536	53.6	307.7
	5	437.0	417.0	104.2	103.8	0.563	56.3	190.6
	10	444.0	256.0	80.2	71.8	0.836	83.6	121.8
	15	442.0	159.0	82.7	78.5	0.883	88.3	72.7
	20	403.0	77.6	91.6	38.8	0.946	94.6	35.5
B	1	376.5	824.0	93.2	136.5	0.114	11.4	376.5
	5	213.9	468.0	171.0	125.7	0.497	49.7	213.9
	10	114.8	351.0	62.4	78.7	0.623	62.3	114.8

	15	136.0	298.0	67.3	90.3	0.680	68.0	136.0
	20	62.9	138.0	99.4	64.7	0.852	85.2	62.9
C	1	530.0	865.0	137.7	222.9	0.700	7.0	418.0
	5	520.0	751.0	124.5	159.3	0.192	19.2	388.9
	10	530.0	576.0	98.4	136.1	0.381	38.1	263.0
	15	444.0	316.0	100.4	86.7	0.660	66.0	122.1
	20	530.0	221.0	45.8	58.3	0.762	76.2	55.1

The anodic Tafel significantly slope improve with the rise in the dose of inhibitor Table 5 that might be ascribed to the exchanges in charge transfer coefficient for the anodic corrosion of SS reaction because the existence of an energy barrier given by the adsorbed inhibitor molecules[53]. It could therefore note that the influence of inhibitor given both the reaction cathodic and anodic of the corrosion process, which means that, investigated assembled study as a mixed type inhibitor in the present case [54, 55]. i_{corr} lowered with rise in the dose of inhibitor and became one order of magnitude break down at an investigated assembled dose of 20 μM . The $\eta_{\text{Tafel}}\%$ was measured from the i_{corr} in existence and non-inhibited of compounds utilized the equation as written elsewhere [56]. Investigated assembled were shown to have very excellent %IE in the acid medium of SS 304 in the experimental attendance of acidic solution Table 5. $\eta_{\text{Tafel}}\%$ improved with rise in the dose of inhibitor. A corrosion protection efficiency of up to 94% was obtained with the utilized of investigated assembled at the dose of the 20 μM .

3.2.2. EIS technique

EIS provides more knowledge on both the capacitive and resistive habitat SS/solution interface and appropriate for in situ and non-destructively probing relaxation phenomena over a range frequency [57]. The EIS values were obtain as typical Nyquist diagrams. These are often utilized in the literature electrochemical due to they allow for an easy measurements of the EIS corrosion elements. The corrosion of SS 304 in acidic solutions in nonexistence and existence of various doses of the investigated compounds utilized this method. Nyquist plots of various inhibitor doses (A) are draw in Fig. 6. All the plots from Fig. 6 appear to be the same with respect to their shape, but they vary significantly in their area. The spectra of the impedance include a Nyquist semicircle kind without appearance of diffusive contribution to the total impedance (Z) which led to that the dissolution goes mainly under charge-transfer control [58-60]. In the existence of inhibitors the diameter of the capacitive loops increases, this indicative of the extent of inhibition of corrosion process, contrary to the decrease of the capacity of double layer (C_{dl}) which is known from next equation [61]:

$$C_{\text{dl}} = 1 / (2 \pi f_{\text{max}} R_{\text{ct}}) \quad (8)$$

The %IE obtained from the EIS measurements are calculated from the relation [62]:

$$\% \eta = [1 - (R_{\text{ct}} / R_{\text{ct}}^0)] \times 100 \quad (9)$$

where R_{ct}^0 and R_{ct} are the resistance of the charge-transfer data in nonexistence and existence inhibitors, respectively. The diameter of the semicircle and also charge transfer of the corrosion process improve with rising dose of investigated inhibitors.

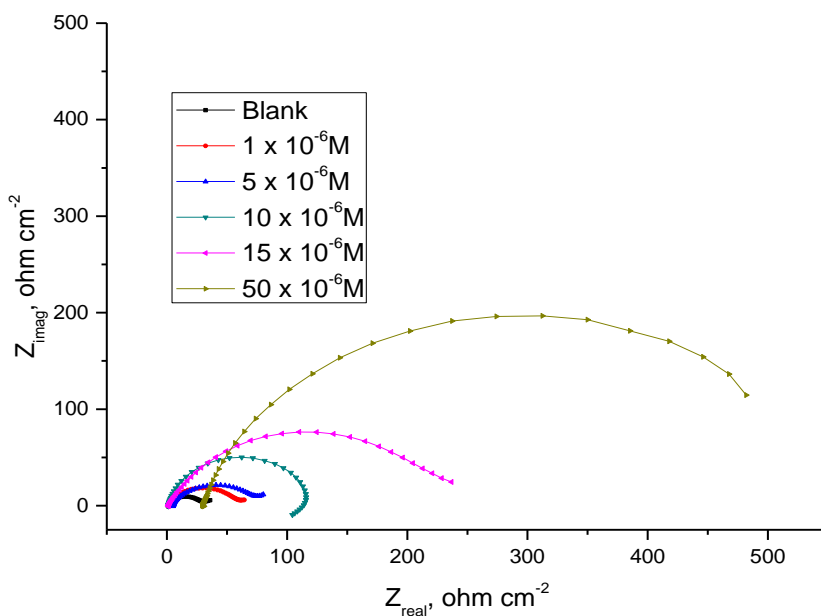


Figure 6. Nyquist curves for 304 SS in nonexistence and existence of various doses of assembled (A).

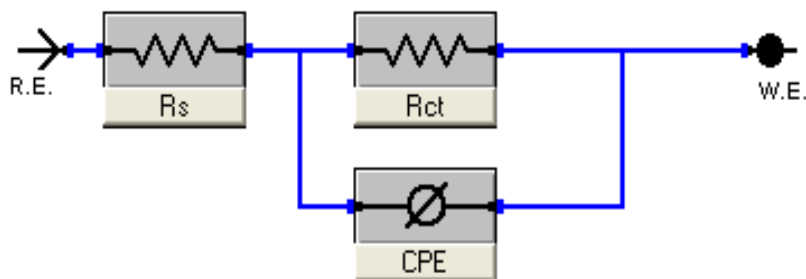


Figure 7. Equivalent circuit utilized to EIS fitting data

Table 6. EIS parameters for SS 304 corrosion in HCl include various doses of investigated inhibitors

Inhibitor	Conc., μM	$C_{dl} \times 10^{-3}, \mu\text{F cm}^{-2}$	$R_{ct}, \Omega \text{ cm}^2$	θ	$\% \eta$
blank	1 M HCl	462.9	29.27	----	----
A	1	269.1	57.5	0.484	48.4
	5	337.1	72.1	0.588	58.8
	10	157.0	114.8	0.741	74.1
	15	476.3	234.5	0.873	87.3
	20	804.5	936.4	0.968	96.8
B	1	363.3	47.5	0.374	37.4
	5	334.4	54.7	0.456	45.6

	10	245.5	73.9	0.598	59.8
	15	188.1	93.6	0.689	68.9
	20	136.0	213.9	0.861	86.1
C	1	317.5	34.6	0.142	14.2
	5	317.4	42.5	0.300	30.0
	10	224.3	53.1	0.441	44.1
	15	338.0	63.7	0.553	55.3
	20	179.2	131.4	0.774	77.4

Due to, the presence of inhibitor rise the adsorption over the surface of SS 304 and obtained data coating layer which may lower the electron transfer among the SS surface and the aggressive medium. On the other side, there is a break down in C_{dl} data along with rising in the dose of the organic assembled. Due to the displacement gradual molecules of water with those of the organic assembled on the surface of electrode leading to a lower in the active center and lower the process of corrosion [63]. The slowing down in the value of C_{dl} , may be ascribed to lower in the local dielectric constant and/or rise in the electrical double layer thickness. As a data, the higher R_{ct} with lower C_{dl} at optimum dose is noted. The higher %IE = 96.8%. The achieved protection by these organic assembled lower in series: $A > B > C$

The %IE obtained from WR, PP and EIS tests are in excellent agreement.

3.2.3. EFM tests

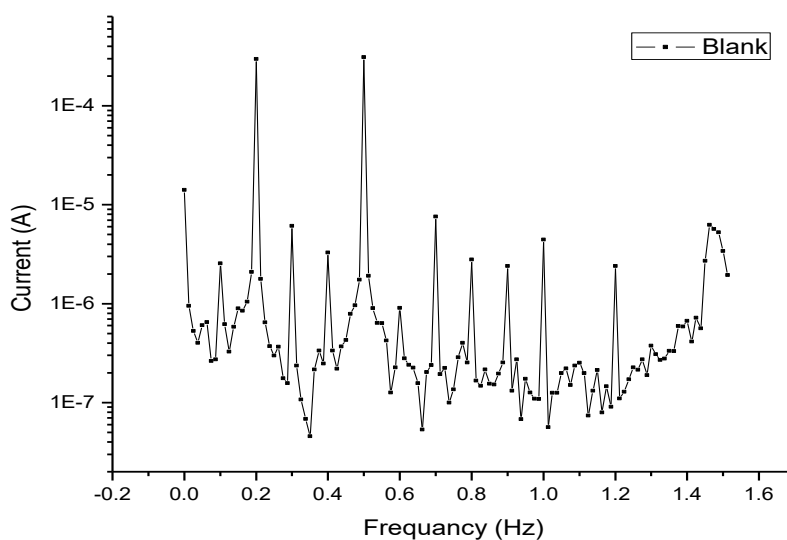


Figure 8. Spectra from EFM for SS 304 in hydrochloric acid (blank).

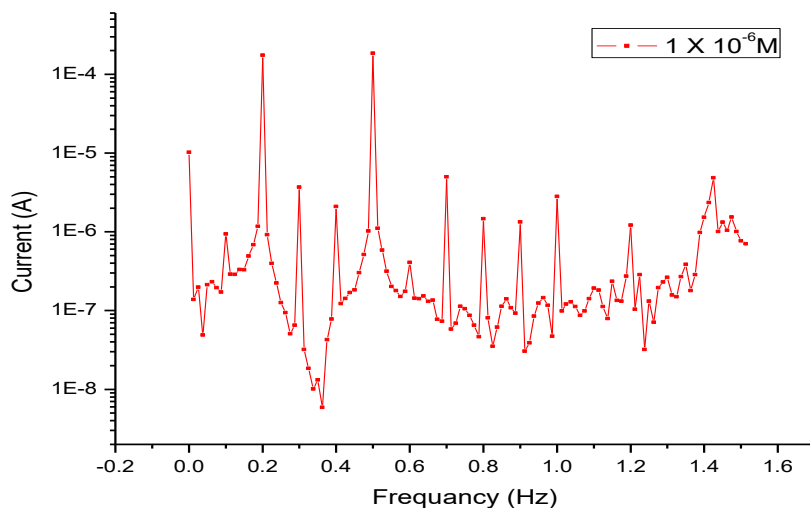


Figure 9. Spectra from EFM for SS 304 in hydrochloric acid in existence of 1×10^{-6} M from inhibitor (A)

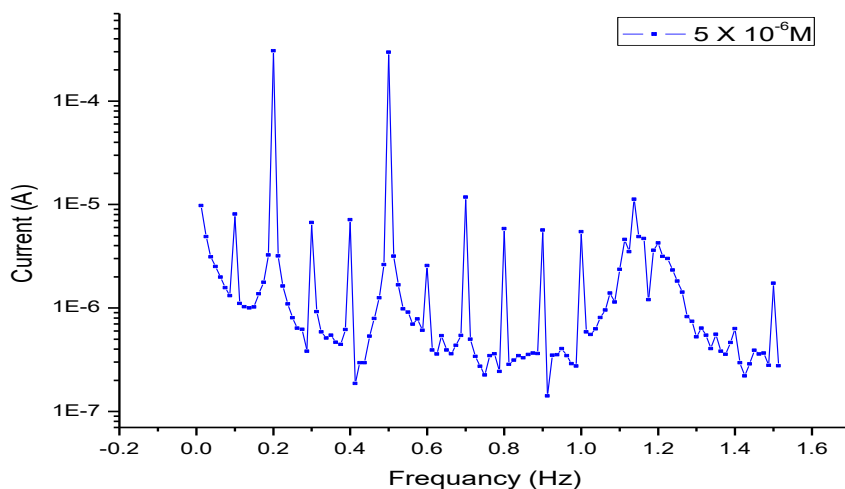


Figure10. Spectra form EFM for SS304 in hydrochloric acid in existence of 5×10^{-6} M from inhibitor (A).

EFM can undertake and quickly calculate the current corrosion data without prior information of Tafel slopes. These important of EFM tests make it real candidate for corrosion online calculation. The causality factors which attend as an internal examine on the exactitude of EFM calculation. The causality factors CF-2 and CF-3 are measure from the current of frequency spectrum. The EFM of SS 304 in HCl solution contain (1, 5, 10, 15 and 20 μM) of organic assembled at 25°C are given in Fig. (8-14).

The intermodulation band and harmonic are apparent visible and are much higher than the noise of background. EFM data were treated utilized two unlike models: perfect control diffusion of the cathodic reaction and the “activation” model. For second, a set of three non-linear equations had been occurs, assuming that the potential of corrosion does not exchange because the polarization of the electrode working [64-66].

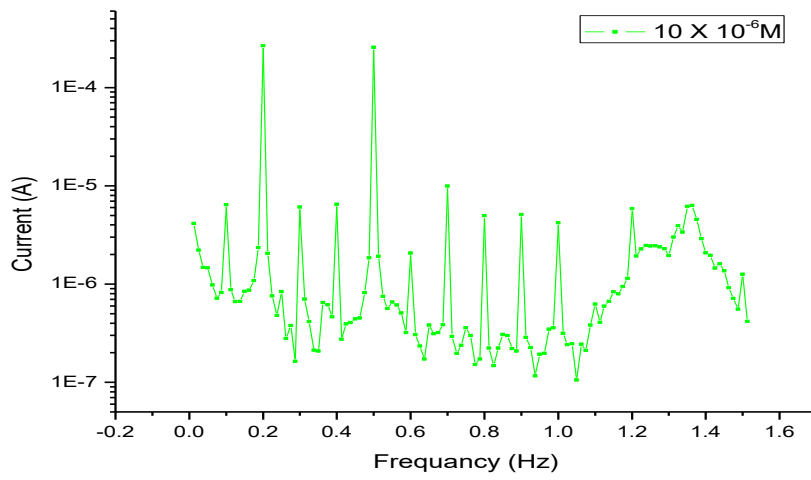


Figure11. Spectra form EFM for SS304 in hydrochloric acid in existance of $10 \times 10^{-6} \text{ M}$ from inhibitor (A)

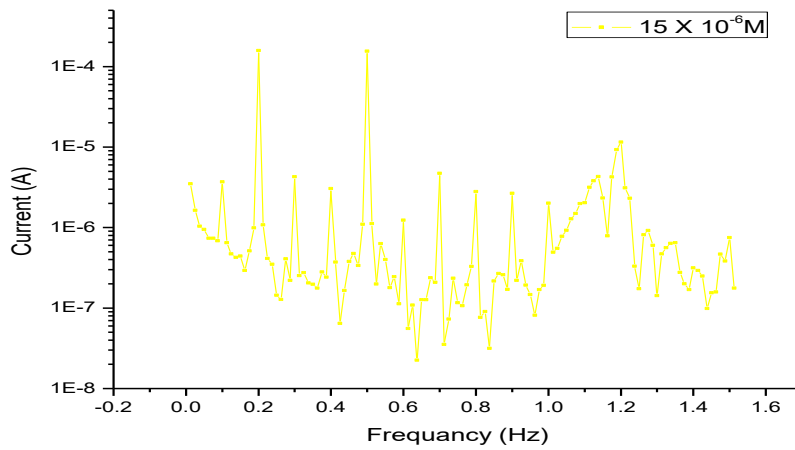


Figure 12. Spectra from EFM for SS 304 in hydrochloric acid in existance of $15 \times 10^{-6} \text{ M}$ from inhibitor (A)

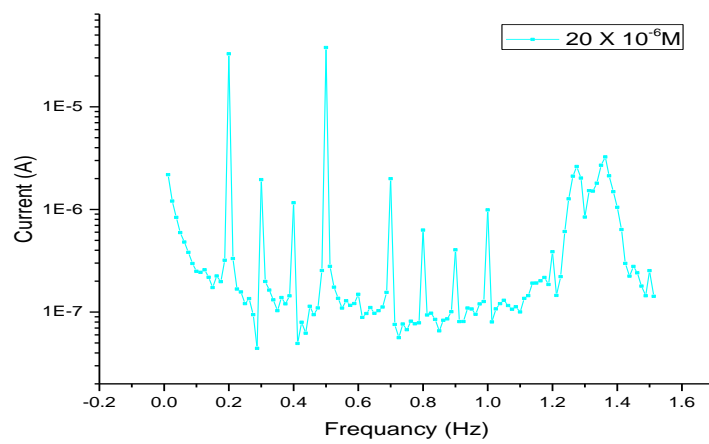


Figure13. Spectra from EFM for SS304 in hydrochloric acid in existance of $20 \times 10^{-6} \text{ M}$ from inhibitor (A)

Table 7. EFM parameters for SS 304 corrosion in HCl including various doses from investigated inhibitors

Inhibitor	Conc., μM	$i_{\text{corr.}}$, $\mu\text{A cm}^{-2}$	β_a , mV dec^{-1}	β_c , mV dec^{-1}	CF-2	CF-3	Θ	% η_{EFM}
Blank	1 M HCl	595.5	140	117	1.78	2.58	-----	-----
A	1	390.1	158	128	1.77	2.61	0.345	34.5
	5	381.7	90	77	1.57	2.77	0.359	35.9
	10	318.7	86	74	1.50	3.25	0.465	46.5
	15	153.4	67	60	1.78	3.20	0.742	74.2
	20	60.41	138	94	1.84	2.78	0.899	89.9
B	1	411.8	148	116	1.81	2.72	0.309	30.9
	5	390.5	103	89	1.58	2.94	0.345	34.5
	10	341.3	90	76	1.53	2.85	0.427	42.7
	15	173.1	94	72	1.88	2.77	0.709	70.9
	20	92.6	95	81	1.50	2.80	0.845	84.5
C	1	496.0	90	78	1.56	3.19	0.167	16.7
	5	422.3	111	136	1.76	2.73	0.291	29.1
	10	381.1	120	158	1.84	2.80	0.362	36.2
	15	272.2	91	77	1.59	2.55	0.593	59.3
	20	179.4	95	81	1.90	2.53	0.699	69.9

The value in Table 7 give that, the appending of any one of tested composite at a given dose to the acidic medium brought down i_{corr} , lead to these composite prevent the SS 304 corrosion in HCl by adsorption. The CF obtain under unlike tests are nearly equal to the theoretical data (2 and 3) lead to that the calculated data are perfect and of best quality. $\% \eta$ improves by raising the inhibitor dose for 304 SS measured from Eq. (7). The measured protection efficiency given from mass reduction, PP and EIS tests are in agreement with that given from EFM tests

3.3. Atomic Force Microscopy (AFM)

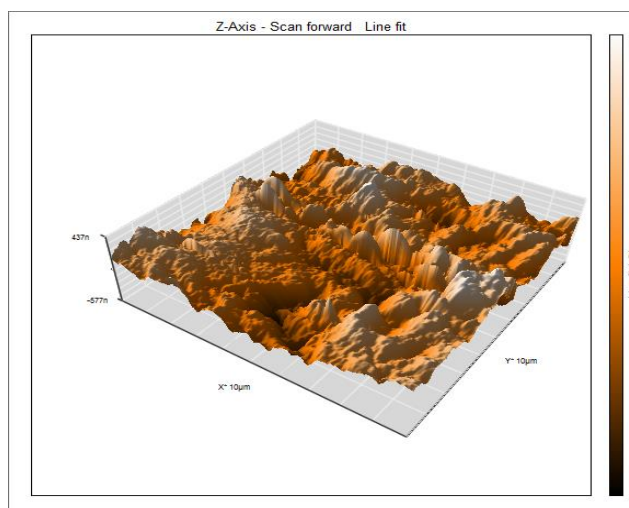


Figure 14. AFM image for SS 304 in 1 M HCl (blank)

AFM analysis is one of the major analyses for surface study, which could be used further investigation in the formation of film coating on the SS 304 surface [67, 68]. The AFM is used to given the topography image of SS 304 in presence and absence of optimum dose of inhibitor. As can be seen from Fig .15 there is much lower damage on the SS 304 surface with investigated inhibitor compared to SS 304 surface immersed in acidic medium solution without inhibitor in Fig .14. AFM parameters are summarized in the Table 8

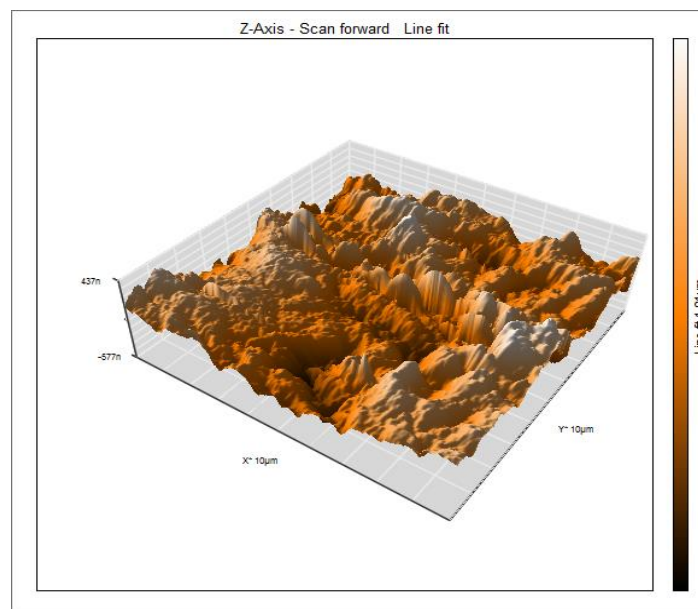


Figure 15. Spectra from AFM for SS 304 in existence of 25×10^{-6} M from inhibitor (A)

Table 8. AFM parameters for SS 304 in HCl in existence and nonexistence of 25 µM of organic inhibitors

Sample	Roughness Sqm (nm)
Polished SS 304	53.159
SS 304 in 1 M HCl	247.690
SS 304 in 1 M HCl + Inhibitor A	144.510
SS 304 in 1 M HCl + Inhibitor B	180.890
SS 304 in 1 M HCl + Inhibitor C	197.610

4. CORROSION PROTECTION MECHANISM

Adsorption of organic compounds which is the essential mechanism of corrosion inhibition which can be explained by two basic kinds of interactions: chemisorptions and physisorption. Organic molecules may be adsorbed on the metal surface in four ways namely: (i) electrostatic interaction between the charged molecules and the charged metal, (ii) interaction of unshared electron pairs in the molecule with the metal, (iii) interaction of π -electrons with the metal, and (iv) donor-acceptor interactions between the π - electrons of aromatic ring and the metal atoms [69]. The adsorption organic derivatives can be attributed to the presence of polar unit having atoms of nitrogen, and oxygen and aromatic rings [70]. Therefore, the possible reaction centers are unshared electron pair of hetero atoms and π -electrons of aromatic ring. It is well known that, the inhibitors have unoccupied orbitals, so exhibit a tendency to accept electrons from d-orbital of metal to form stable chelates which are considered as excellent inhibitor [71].

The order of lowering protection efficiency due to first inhibitor (A) has excellent protection efficiency due to: i) its higher molecular size (371.43) that may facilitate better adsorption on the SS 304 surface and hence, it covers larger molecular area, ii) also it has 3-N, 3-O and 2-S atoms and 2 benzene rings which serve as adsorption centers. Substance (B) comes after substance (A) in % η due to: i) it has lower molecular size (337.13) and ii) it has 5-N and 3-O atoms no S-atoms and 2 benzene rings (S > N > O in the basicity). Inhibitor (C) is the least effective substance in protection efficiency due to: i) it has lesser molecular size (308.38) and ii) also it has 2-N, 3-O and 2-S atoms and one benzene ring.

5. CONCLUSIONS

The investigated inhibitors show good performance as corrosion protection in acidic solution. The protection efficiency of organic assembled follows the sequence: A > B > C. PP research given that investigated assembled behave as mixed kind inhibitors for SS 304 in acidic medium. Impedance tests led to that R_{ct} value raised, while break down C_{dl} data in the existence of the inhibitors. The adsorption of the organic compounds followed the Temkin adsorption isotherm which led to the protection process take place by adsorption. The % η given from WR, PP tests, EIS and EFM are in excellent agreement

References

1. M. Behpour, S.M. Ghoreishi, N. Soltani, M. Salavati-Niasari, *Corros. Sci.*, 51 (2009) 1073.
2. M. Behpour, S.M. Ghoreishi, M. Khayat Kashani, N. Soltani, *Mater. Corros.* 60 (2009) 895.
3. F. Eghbali, M.H. Moayed, A. Davoodi, N. Ebrahimi, *Corros. Sci.*, 53 (2011) 513.
4. M. Abdallah, *Corros. Sci.*, 44 (2002) 717.
5. A.S. Fouda, A.S. Ellithy, *Corros. Sci.* 51 (2009) 868.
6. S.A.M. Refaey, F. Taha, A.M. Abd El-Malak, *Appl. Surf. Sci.*, 236 (2004) 175.

7. A.S. Fouda, M. Abdallah, S.M. Al-Ashrey, A.A. Abdel-Fattah, *Desalination*, 250 (2010) 538.
8. R. Fuchs-Godec, *Electrochim. Acta*, 54 (2009) 2171.
9. N. Caliskan, E. Akbas, *Mater. Chem. Phys.*, 126 (2011) 983.
10. F. Bentiss, M. Traisnel, M. Lagrennee, *Corros. Sci.*, 42 (2000) 127.
11. L. Elkadi, B. Mernari, M. Traisnel, F. Bentiss, M. Lagrennee, *Corros. Sci.*, 42 (2000) 703.
12. R. Walker, Triazole, *Corros. Sci.*, 31 (1975) 97.
13. F. Bentiss, M. Lagrennee, M. Traisnel, J.C. Lornez, *Corros. Sci.*, 41 (1999) 789.
14. T.P. Zhao, G.N. Mu, *Corros. Sci.*, 41 (1999) 1937.
15. C. Cao, *Corros. Sci.* 38 (1996) 2073.
16. F. Bentiss, M. Traisnel, H. Vezin, H.F. Hildebrand, M. Lagrennee, *Corros. Sci.*, 46 (2004) 781.
17. F. Zucchi, G. Trabanelli, G. Brunoro, *Corros. Sci.*, 36 (1994) 1683.
18. F. Bentiss, M. Lagrennee, M. Traisnel, J.C. Hornez, *Corrosion*, 55 (1999) 968.
19. S. Ali, M. Saeed, S. Rahman, *Corros. Sci.*, 45 (2003) 53.
20. A. Fouda, A. Al-Sarawy, M.S. Radwan, *Annali di Chimica*, 96 (2006) 85.
21. A. Fouda, F. El-Taib Heakal, M. Radwan, *J. Appl. Electrochem.* 39 (2009) 391
22. D. Karthik, D. Tamilvendan, G. Venkatesa Prabhu, *Journal of Saudi Chemical Society* (2014) 18, 835–844
23. W.B. Ken, L.L. Li, Z. Wang, *Corrosion and Protection*, 32(10) (2011) 765
24. J. Nie, Y. Si, Q. Yu, Z. Wang, *Corros. Sci. Prot. Technol.*, 23(5) (2011) 422
25. J. Zhao, G. Cui, *Int. J. Electrochem. Sci.*, 6(9) (2011) 4048
26. R. Herle, P. Shetty, S.D. Shetty, U.A. Kini, *Port. Electrochim. Acta*, 29(2) (2011) 69
27. R. Zhao, X. Tang, Y. Zuo, *Corros. Sci. Protection Technol.*, 23(3) (2011) 251
28. K. Yoo, K. Chung, N.K. Kim, *Industrial and Engineering Chemistry Research*, 52(32) (2013) 10880
29. J.J. Jacob, R.S. Kannan, A. Jawahar, *Corros. Sci.*, 47(1) (2013) 1009
30. B. Rao, M. Rao, S. Rao, B. Sreedhar, *J. Surf. Eng. Mater. Adv. Technol.*, 3(1) (2013) 28
31. J.A. Thangakni, S. Rajendran, J. Sathiyabama, J.I. Chisty, A.S. Prabha, M. Pandiarajan, *European Chemical Bulletin*, 1(5) (2013) 265
32. S. Gowri, J. Sathiyabama, P. Prabhakar, S. Rajendran, *Int. J. Res. Chem. Environ.*, 3(1) (2013) 156
33. E. Caaffery, *Science press, Princeton*, 1979.
34. B. Al-Anadoui, F. Elnizami, B. Ateya, *Extended Abstract of the Electrochemical Society Fall Meeting*, Chicago, 1988, pp. 188.
35. J. Borkirs, D. Swinkless, *J. Electrochem. Soc.*, 111 (1964) 136.
36. M. Temkin, Z. Khim, 15 (1941) 296.
37. M. Abdallah, A. Fouda, S. Shama, E. Afifi, *African J. Pure Appl. Chem.*, 2 (9) (2008) 83.
38. X. Li and G. Mu, *Appl. Surf. Sci.*, 252 (2005) 1254.
39. A. A. El-Awady, B. Abd El-Nabey and S. G. Aziz, *Electrochem. Soc.*, 139 (1992) 2149.
40. L. Tang, X. Li, Y. Si, G. Mu and G. Liu, *Mater. Chem. Phys.*, 95 (2006) 29.
41. L. Tang, G. Murad and G. Liu, *Corros. Sci.*, 45 (2003) 2251.
42. I. Putilova, S. Balezin, I. Barannik, and V. Bioshop, in *Metallic Corrosion Inhibitors Oxford: Pergamon*, (1960) 196.
43. K. Haladhy, L. Collow and J. Dwanson, *Br. Corros. J.*, (1980) 15.
44. W. Durine, R.D. Marco, A. Jefferson and B. Kinsella, *J. Electrochem. Soc.*, 146 (1999) 1751.
45. R. Casparac, C.R. Martin and E.J. Stupnisek – Lisac, *Electrochem. Soc.*, 147(2) (2000) 548.
46. A. Fouda, M. Gouda and S. Abd El-Rahman. *Bull. Korean Chem. Soc.*, 21(1) (2000) 1085.
47. G. Quartarone, M. Battilana, L. Bonaldo and T. Tortato, *Corros. Sci.*, 50 (2008) 3467.
48. E. Oguzie, *Corros. Sci.*, 49 (2007) 1527.
49. J. Talate, M. Desai and N. Shah, *Anti-Corros. Meth. Mater.*, 52(2) (2009) 108.
50. S. Martinez and M. Matikos-Hukoric, *J. Appl. Electrochem.*, 33 (2003) 1137.
51. O. Riggs and R. Hurd, *Corrosion*, 23 (1967) 252.
52. M. Gomma and M. Wahdan, *Mater. Chem. Phys.*, 39 (1995) 209.

53. G. Quartarone, G. Moretti, A. Tassan, A. Zingales, *Werkst. Korrosion*, 45 (1994) 641.
54. M. Abdel-aal, M. Morad, Br. *Corros. J.*, 36 (4) (2001) 253.
55. G. Quartarone, L. Bonaldo, C. Tortato, *Appl. Surf. Sci.*, 252 (23) (2006) 8251.
56. B. Hammouti, E. Chaieb, A. Bouyanzer, M. Benkaddour, *Appl. Surf. Sci.*, 246 (1–3) (2005) 199.
57. S. Mertens, C. Xhoffer, B. Decooman, E. Temmerman, *Corrosion*, 53 (1997) 381.
58. J. Hu, X. Liu, J. Zhang, C. Cao, *Prog. Org. Coat.*, 55 (2006) 388.
59. K. Shimizu, A. Lasia, J. Boily, *Langmuir*, 28 (2012) 7914.
60. M. Motamedi, A. Tehrani-Bagha, M. Mahdavian, *Electrochim. Acta*, 58 (2011) 488.
61. P. Agarwal, M. Orazem, L. Garcia-Rubio, *J. Electrochem. Soc.*, 139 (1992) 1917.
62. J. Ross. Macdonald, Impedance, Spectroscopy, *Jon Wiley and Sons*, (1987)
63. S. Abd El-Rehim, A. Magdy and K. Khaled, *J. Appl. Electrochem.*, 29 (1999) 593
64. M. Outirite, M. Lagrenee, M. Lebrini, M. Traisnel, C. Jama, H. Vezin, F. Bentiss, *Electrochim. Acta*, 55 (2010) 1670.
65. K. Khaled and M. Amin, *Corros. Sci.*, 51 (2009) 1964.
66. E. Kus, F. Mansfeld, *Corros. Sci.*, 48 (2006) 965.
67. M. Bethencourt, F. Botana, J. Calvino, M. Marcos, *Corros. Sci.* 40 (1998) 1803.
68. V. Otieno- Alego and G. Hope, *Corros. Sci.*, 33 (1992) 1719
69. A. K. Singh and M.A. *Corros. Sci.*, 52 (2010) 152.
70. S. S. Abd El-Maksoud and H.H. Hassan, *Mater. Corros.* 58 (2007) 369.
71. S. L. Li, Y.G. Wang, S.H. Chen, R. Yu, S.B. Lei, H.Y. Ma, and D.X. Lin, *Corros. Sci.* 41 (1999) 1769.

© 2017 The Authors. Published by ESG (www.electrochemsci.org). This article is an open access article distributed under the terms and conditions of the Creative Commons Attribution license (<http://creativecommons.org/licenses/by/4.0/>).